Jet Propulsion Laboratory
California Institute of Technology

Low-CNR inverse synthetic aperture LADAR imaging demonstration with atmospheric turbulence

4/19/2016

Russell Trahan, Bijan Nemati, Hanying Zhou,
Michael Shao, Inseob Hahn, William B. Schulze

Presented by Russell Trahan

Jet Propulsion Laboratory
California Institute of Technology

Summary

Goals:

- Demonstrate ISAL functionality in photon-starved conditions.
- Find a metric that can predict the success/failure of PGA based on the return signal strength.

Outline:

- Testbed hardware setup and data processing
  - Basic setup for low-CNR
  - Atmospheric turbulence synthesis
  - Data pipeline
- CNR
  - CNR definition for a single range-bin (including detector noise)
  - Various metrics based on CNR
  - Image quality metric to compare to metrics based on CNR
- Experimental Data
  - High CNR functionality tests
  - Low CNR imaging examples showing PGA failure at mean CNR=~0.25

Jet Propulsion Laboratory
California Institute of Technology

Testbed Hardware Setup and Data Processing

Jet Propulsion Laboratory
California Institute of Technology

Transceiver / Target Layout

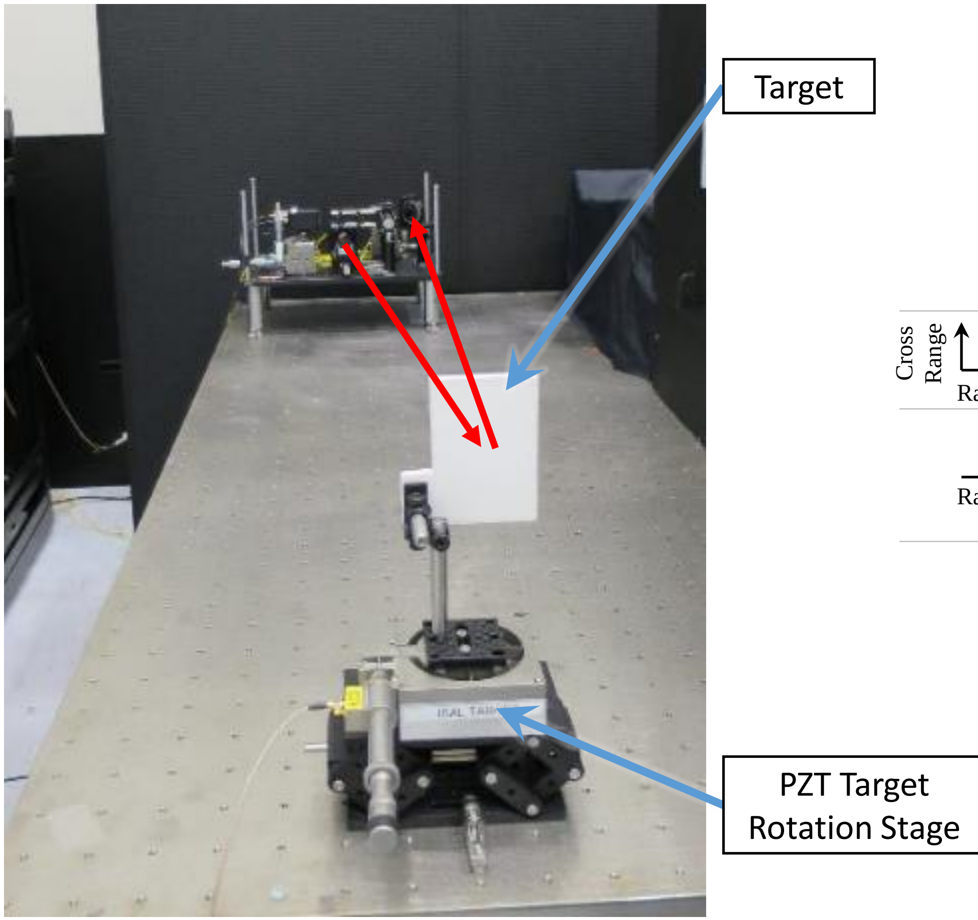

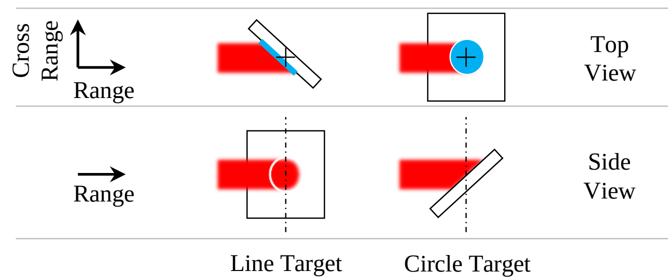

Jet Propulsion Laboratory
California Institute of Technology

Transceiver Assembly

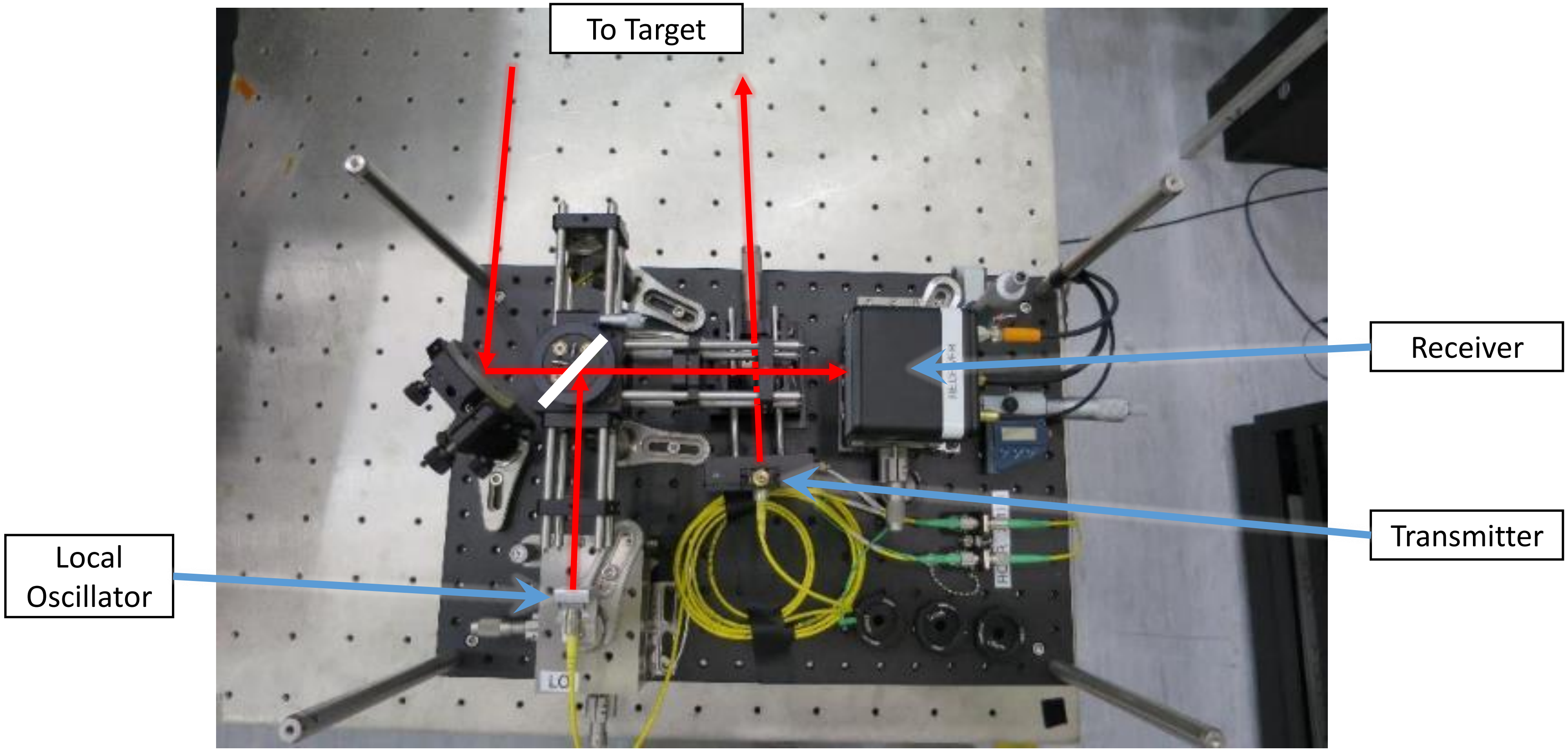

Jet Propulsion Laboratory
California Institute of Technology

Transmitter Designs

- No atmospheric turbulence
  - Fiber termination and collimating lens
- Atmospheric turbulence
  1. Fiber Termination
  2. Collimating Lens – collimate light from fiber
  3. Iris – truncate Gaussian beam to FWHM
  4. Focusing Lens – focus collimated light through the phase wheel
  5. Phase Wheel – introduce phase error
  6. Speckle Image – focal point of focusing lens
  7. Magnification Lens – magnify the speckle image onto the target

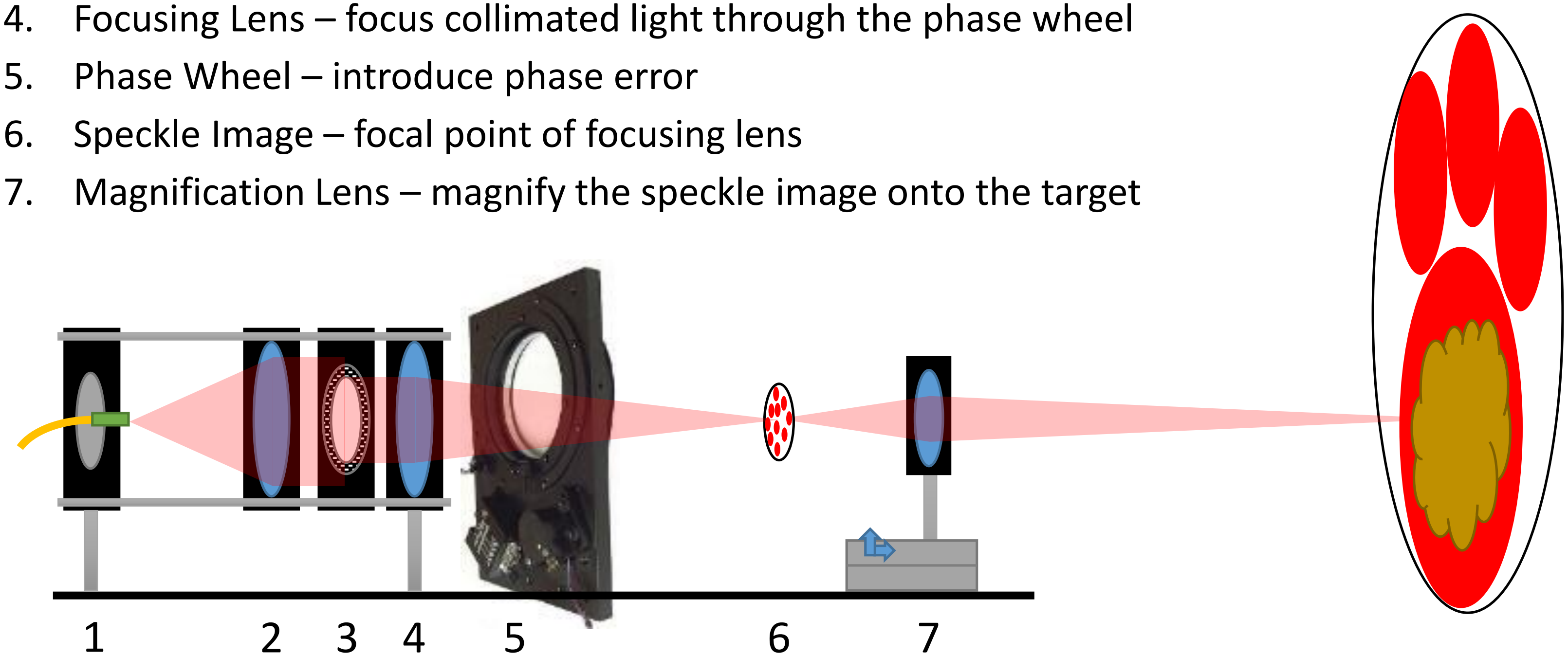

Jet Propulsion Laboratory
California Institute of Technology

Testbed Overview

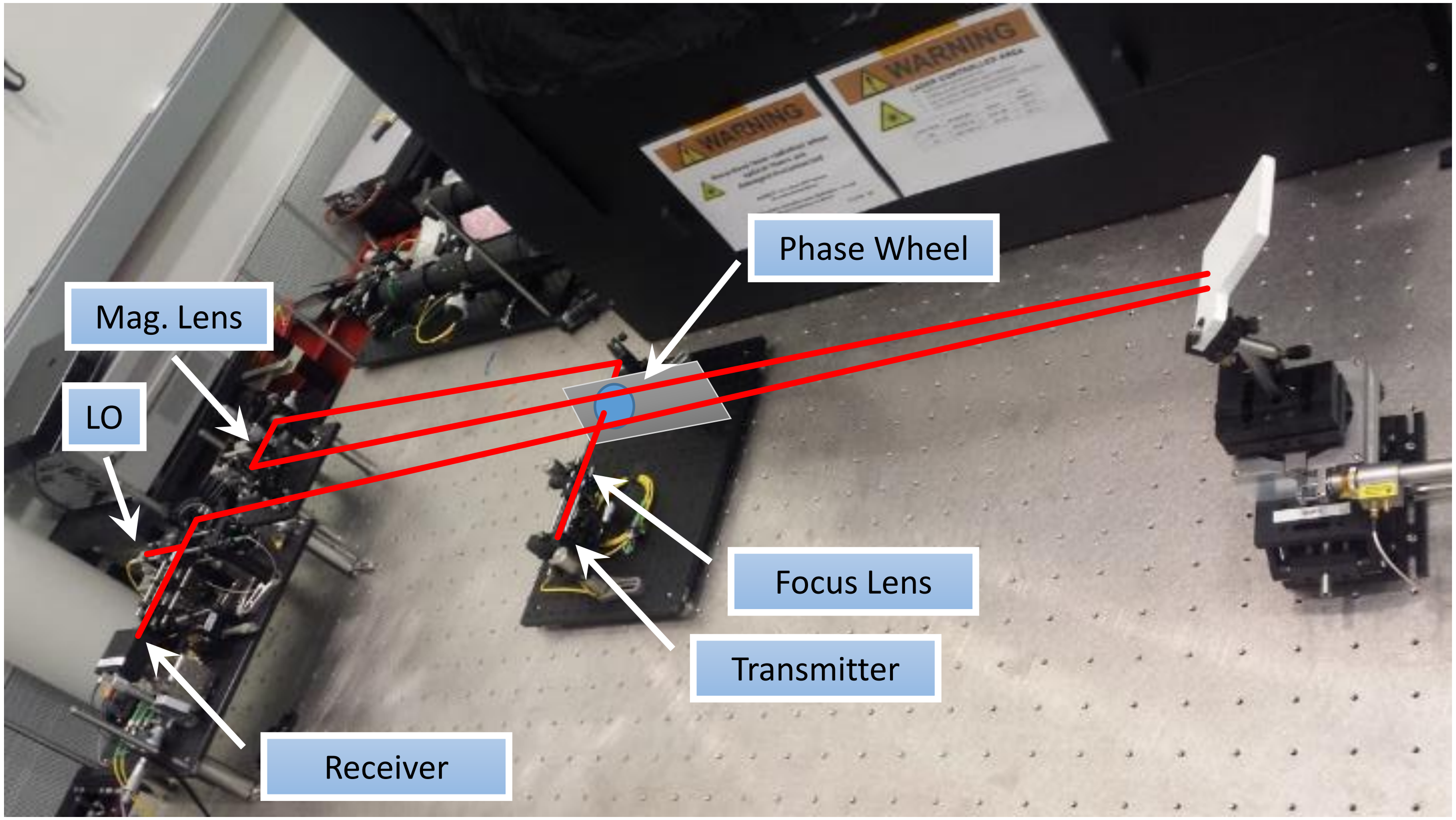

Jet Propulsion Laboratory
California Institute of Technology

PGA Summary

Our best results came from starting the window at 75% of the cross range extent, allowing $\tilde{\varphi}$ to converge to nearly zero, then decreasing window size by 25%. Repeat until window is ~10 pixels in cross range.

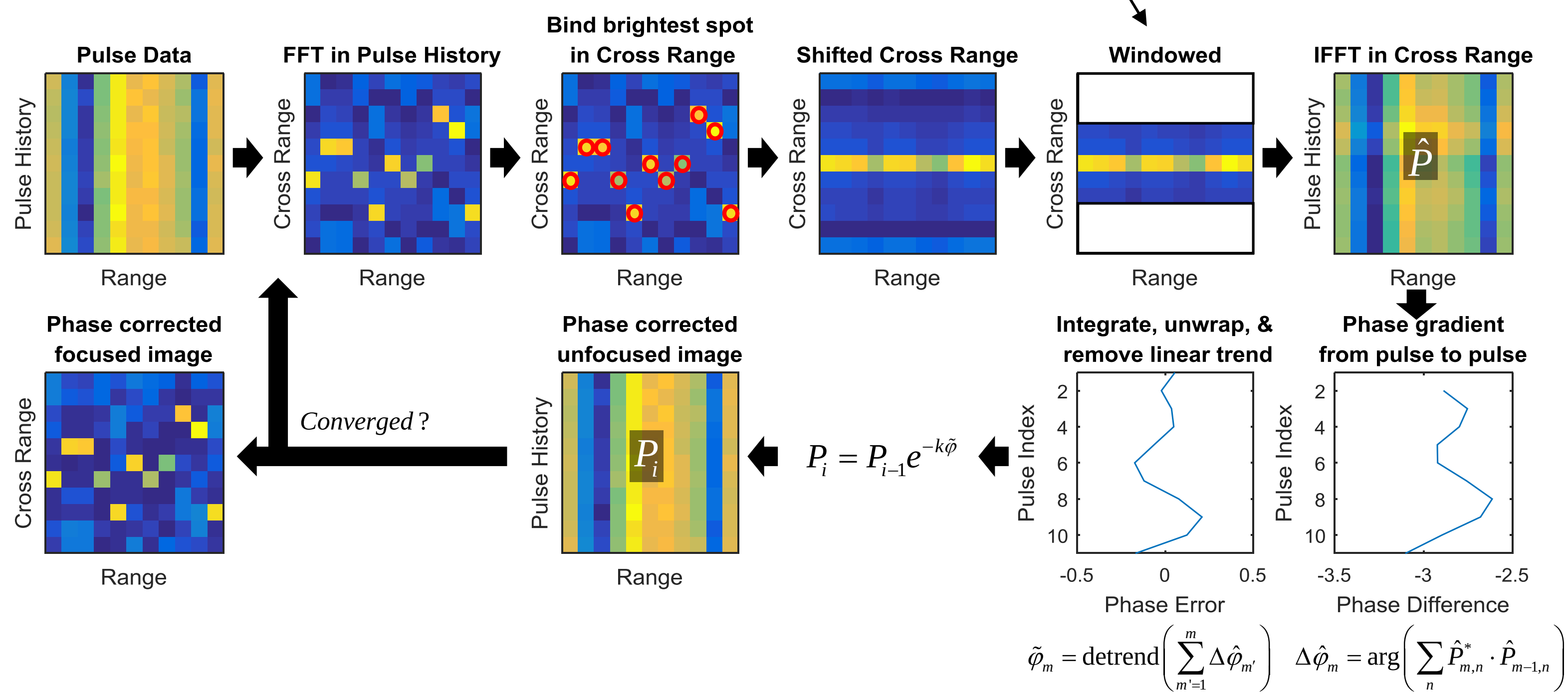

Over-sampling in range or including range-bins with very low CNR shouldn't influence the phase increments. Simply includes noise in summation.

Jet Propulsion Laboratory
California Institute of Technology

CNR Derivation and Image Quality Metrics

Jet Propulsion Laboratory
California Institute of Technology

CNR Definition

- CNR is defined as $\dfrac{\text{Estimate of carrier strength}}{\text{StdDev of estimate of carrier strength}}$
- Measurement can be modeled as

$$\eta_d \sqrt{\eta_h N_L \tilde{N}_S} \exp(i\varphi) = \eta_d \sqrt{\eta_h N_L N_S} \exp(i\varphi_s) + N\left(0, \sigma_{SN}^2\right) + N\left(0, \sigma_{NEP}^2\right)$$

  - The carrier for a single range bin is $\eta_d \sqrt{\eta_h N_L N_S} \exp(i\varphi_s)$
  - Shot noise variance is $\sigma_{SN}^2 \approx \eta_d \dfrac{N_L}{2}$
  - Detector NEP noise variance is $\sigma_{NEP}^2 = \dfrac{P_{NE}^2 \tau}{2h^2 \nu^2}$
- Model is used to estimate the carrier strength and its variance

$$CNR = \frac{\left\langle N_L \tilde{N}_S \right\rangle}{\sqrt{\operatorname{var}\left(N_L \tilde{N}_S\right)}} = \frac{N_S}{\sqrt{\dfrac{2N_S}{\eta_d \eta_h} + \dfrac{1}{\eta_d^2 \eta_h^2} + \dfrac{4N_S \sigma_{NEP}^2}{\eta_d^2 \eta_h N_L} + \dfrac{4\sigma_{NEP}^2}{\eta_d^4 \eta_h^2 N_L} + \dfrac{4\sigma_{NEP}^4}{\eta_d^4 \eta_h^2 N_L}}}$$

$$CNR = \frac{N_S}{\sqrt{\dfrac{2N_S}{\eta_d \eta_h} + \dfrac{1}{\eta_d^2 \eta_h^2}}} \approx \sqrt{\frac{\eta_d \eta_h N_S}{2}} \text{ for } N_S >> 1/\eta_d \eta_h$$

$$\approx \eta_d \eta_h N_S \text{ for } N_S << 1/\eta_d \eta_h$$

R. L. Lucke and L. J. Rickard, "Photon-limited synthetic-aperture imaging for planet surface studies planet surface studies," *Applied Optics,* vol. 41, no. 24, pp. 5084-5095, 2002.

Quality Metric Selection

Quality metrics based on pre-PGA data:

- # Photons in each range-bin
  Maximum, Mean, Sum, Sum of squares
- CNR of mean photons per range-bin
- CNR of each range-bin
  Maximum, Mean, Sum, Sum of squares
- Phase progression Variance of each range-bin
  Minimum, Mean, Sum, Sum of squares

Quality metric based on post-PGA result:

- Image Contrast-to-Noise Ratio
- $C = \frac{\text{mean(foreground)} - \text{mean(background)}}{\text{stdev(background)}}$
- Foreground region is determined based on a priori knowledge of the target.
- PGA performance cannot be assessed as C decreases past 1.

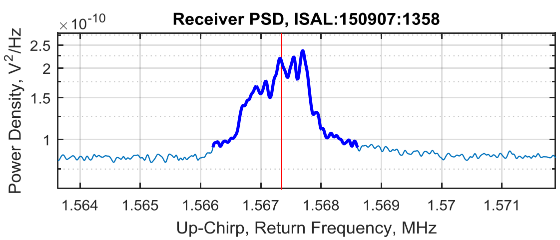

Primary Question:
What quality metric has a consistent value at the threshold where <u>PGA doesn't work</u>?

Immediate Question:
What quality metric has a consistent value when the <u>image contrast-to-noise ratio is 1</u>?

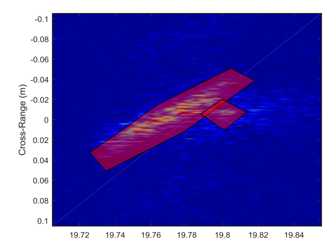

Contrast depends on Cross-Range Extent

Considering only a single range bin and a consistent CNR:

- The image contrast is inversely proportional to the number of cross-range bins populated by the target.
- Parseval's Theorem: $\sum_{n=0}^{N-1} |P_n|^2 = \frac{1}{N} \sum_{k=0}^{N-1} |p_k|^2$
- Sum of a single range-bin's magnitude over all pulses must equal the mean of the cross-range pixel values.
    - If a **single cross-range pixel** is filled by the target, **contrast will be high**.
    - If **several cross-range pixels** are filled by the target, **contrast will be low**.

*This idea is confirmed in the experimental data presented later.

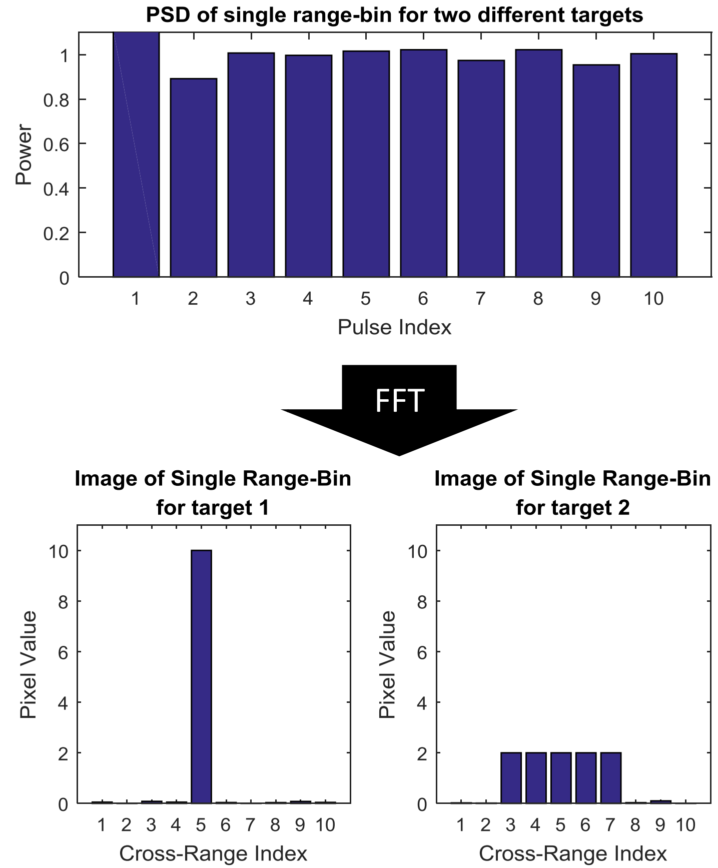

Jet Propulsion Laboratory
California Institute of Technology

Imaging Examples ~2m Range to Target

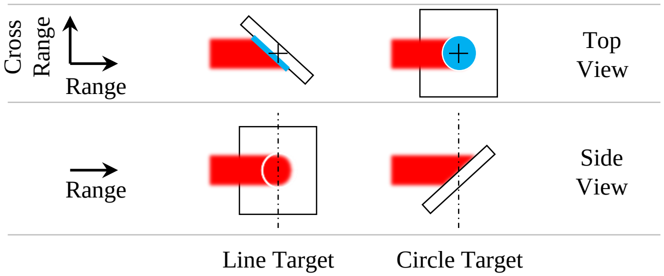

Jet Propulsion Laboratory
California Institute of Technology

Sample Low CNR Result

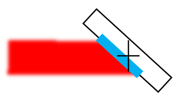

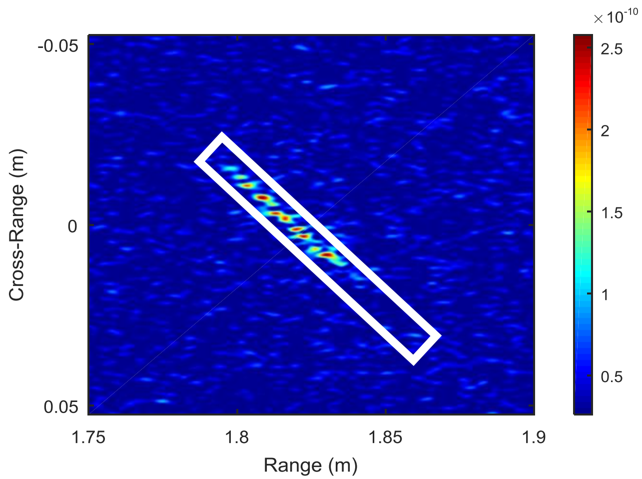

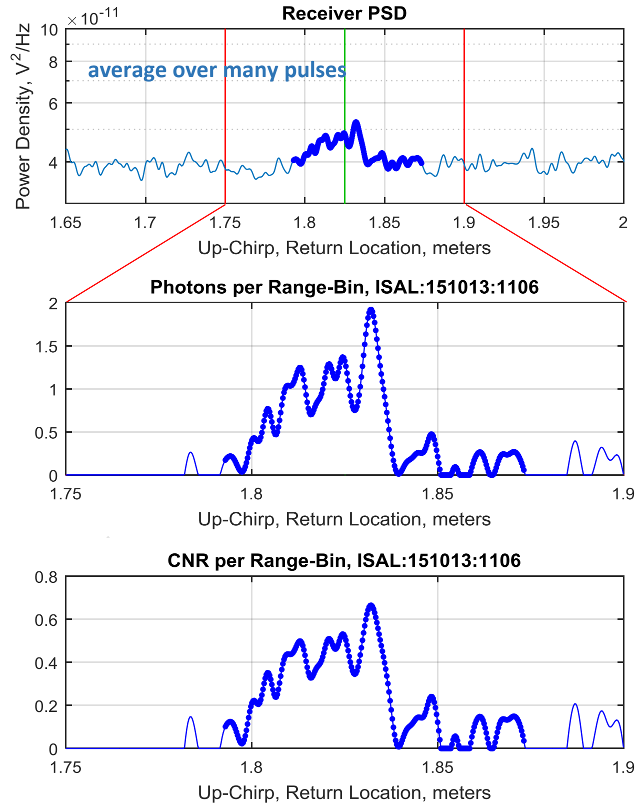

Contrast: 1.9
LO Photons per pulse: 5.05e+12
Range Bins: 33.9

Photons per Range Bin:
- **Max: 1.92**
- **Mean: 0.55**
- Sum: 18.54
- Sum of sqr: 18.52

CNR of Mean Photons per Range Bin: 0.27

CNR of Active Range Bins:
- **Max: 0.66**
- **Mean: 0.24**
- Sum: 8.15
- Sum of sqr: 3.14

Difference

JPL Logo on Spectralon

Chirp Rate	2THz/s
Pulse Length	34 ms
Acq Time	60 s
Mean CNR	2.76

Front View

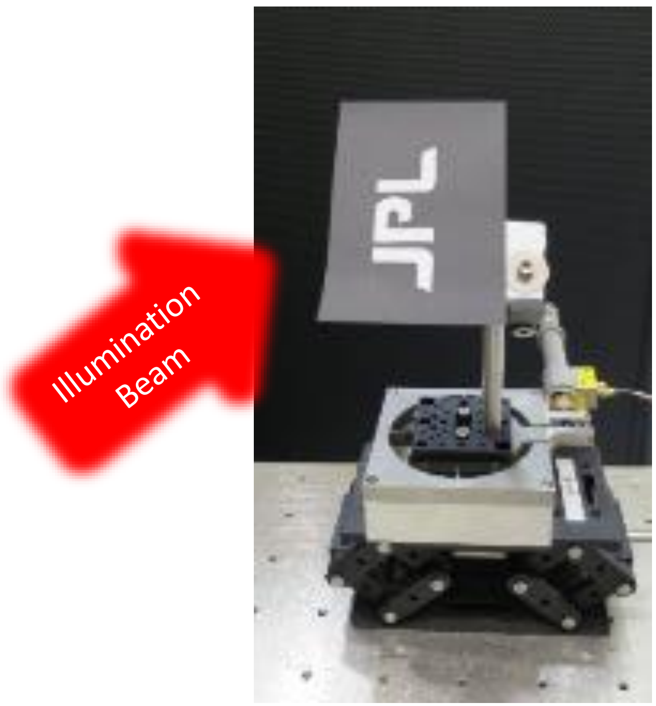

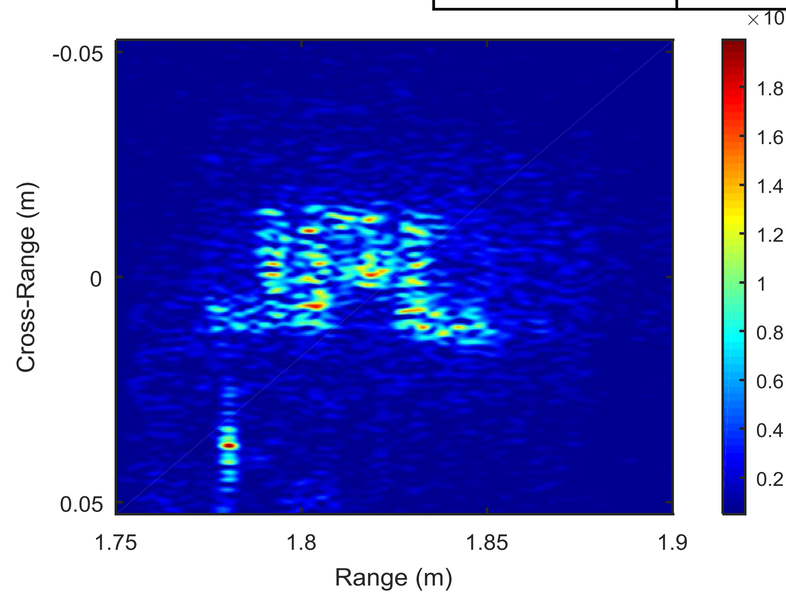

Satellite Image

Chirp Rate	2THz/s
Pulse Length	34 ms
Acq Time	60 s
Mean CNR	4.5

Top View

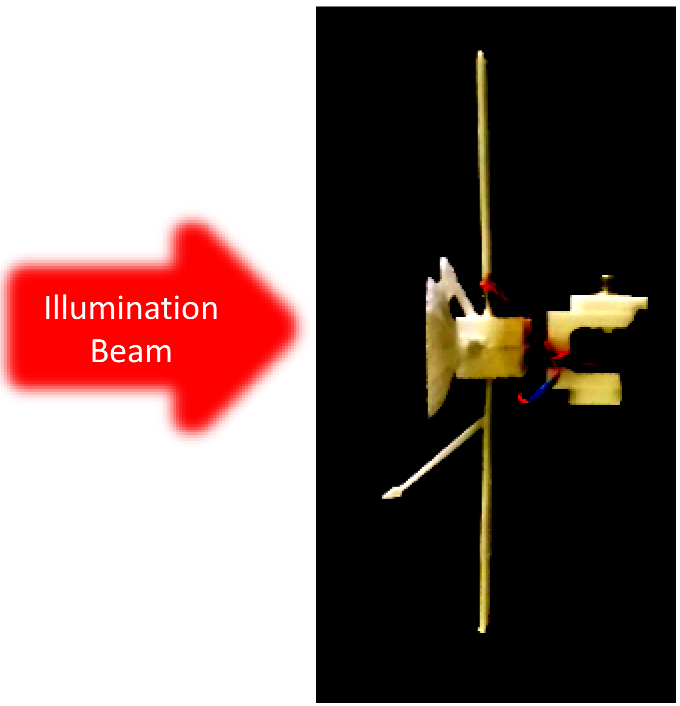

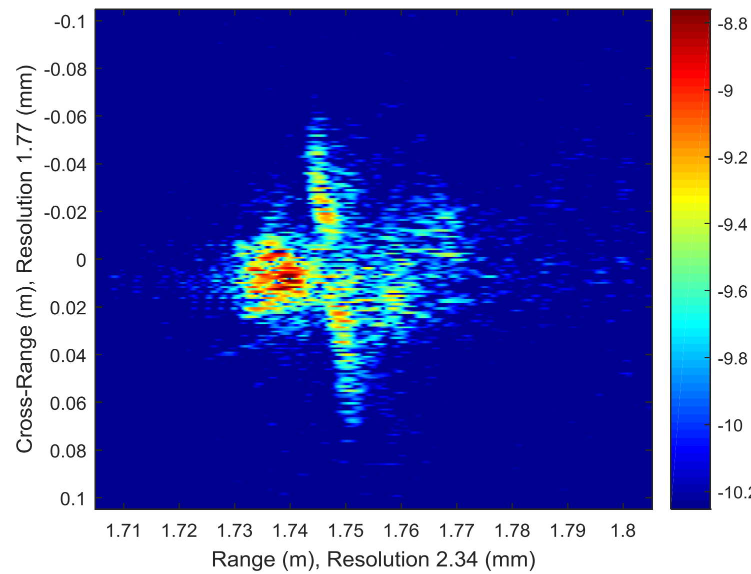

Jet Propulsion Laboratory
California Institute of Technology

Contrast vs Mean CNRs

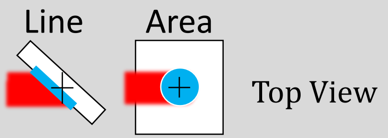

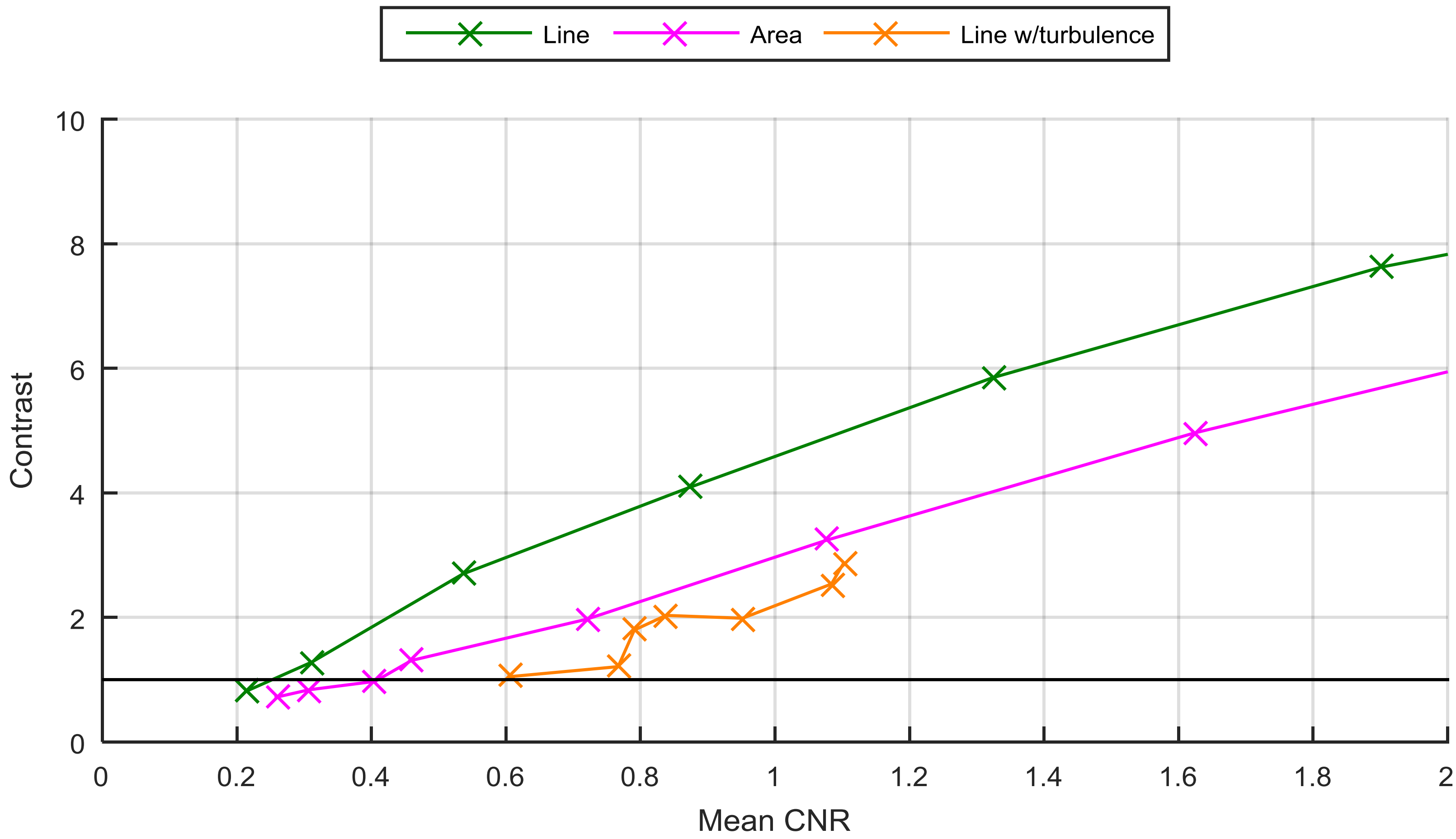

Jet Propulsion Laboratory
California Institute of Technology

Low Mean CNR Images

Line Target (top row)
Area Target (bottom row)

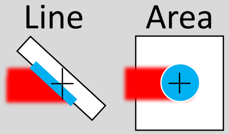

Top View

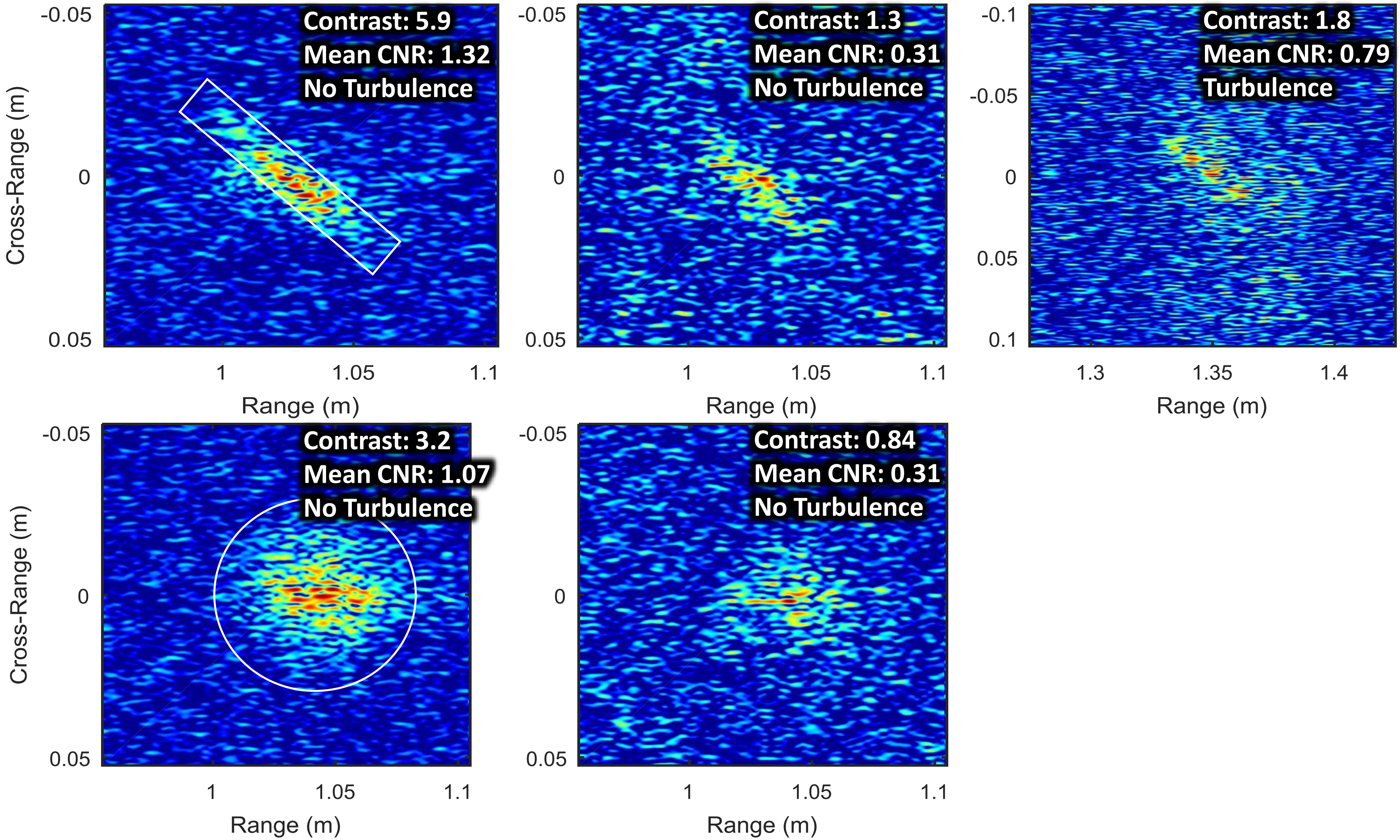

Jet Propulsion Laboratory
California Institute of Technology

Conclusions

- Testbed build to perform ISAL studies
  - Short 2m or long 400m range-to-target
  - Synthesized atmospheric turbulence
  - High and very low CNR capabilities
- CNR Derivation
  - Rigorous derivation of CNR for a single range-bin
  - Quality metric for overall signal: “Mean CNR”
  - Quality metric for image: Contrast-to-Noise Ratio
- Experimental Results
  - Target cross-range extent decreases image contrast (for constant CNR)
  - PGA can work for simple images down to ~0.25 CNR
  - Atmospheric turbulence raises minimum CNR threshold to ~0.75

Sponsors

Jet Propulsion Laboratory
California Institute of Technology

AFRL
THE AIR FORCE RESEARCH LABORATORY
LEAD | DISCOVER | DEVELOP | DELIVER

References

1. Barber, Z. W. and Dahl, J. R., "Synthetic aperture ladar imaging demonstrations and information at very low return levels," Applied Optics 53(24), 5531-5537 (2014).
2. McManamon, P. F., "Review of ladar: a historic, yet emerging, sensor technology with rich phenomenology," Optical Engineering 51(6), 1-13 (2012).
3. Luo, H., Yuan, X. and Zeng, Y., "Range accuracy of photon heterodyne detection with laser pulse based on Geigermode APD," Optics Express 21(16), 18983-18993 (2013).
4. Andrews, A. K., Hudson, R. S. and Psaltis, D., "Optical-radar imaging of scale models for studies in asteroid astronomy," Optics Letters 20(22), 2327-2329 (1995).
5. Harris, A. W., Young, J. W., Conteiras, L., Dockweiler, T., Belkora, L., Salo, H., Harris, W. D., Bowell, E., Poutanen, M., Binzel, R. P., Tholen, D. J. and Want, S., "Phase relations of high albedo asteroids: The unusual opposition brightening of 44 Nysa and 64 Angelina," Icarus 81(2), 365-374 (1989).
6. Mishchenko, M. I. and Dlugach, J. M., "Coherent backscatter and the opposition effect for E-type asteroids," Planetary and Space Science 41(3), 173-181 (1993).
7. Pellizzari, C. J., Bos, J., Spencer, M. F., Williams, S., Williams, S. E., Calef, B. and Senft, D.C., "Performance characterization of Phase Gradient Autofocus for Inverse Synthetic Aperture LADAR," IEEE Aerospace Conference, 1-11 (2014).
8. Lucke, R. L. and Rickard, L. J., "Photon-limited synthetic-aperture imaging for planet surface studies planet surface studies," Applied Optics 41(24), 5084-5095 (2002).
9. Lucke, R. L., Rickard, L. J., Bashkansky, M., Reintjes, J. and Funk, E. E., "Synthetic aperture ladar (SAL): Fundamental theory, design equations for a satellite system, and laboratory demonstration," Naval Research Laboratory, Washington DC, (2002).
10. Gatt, P., Jacob, D., Bradform, B. and Krause, B., "Performance bounds of the phase gradient autofocus algorithm for synthetic aperture ladar," Proc. SPIE 7323, (2009).
11. Falletti, E., Pini, M. and Presti, L., "Low complexity carrier-to-noise ratio estimators for GNSS digital receivers," IEEE Transactions of Aerospace and Electronic Systems 47(1), 420-437 (2011).
12. Sharawi, M. S., Akos, D. M. and Aloi, D. N., "GPS C=N0 estimation in the presence of interference and limited quantization levels," IEEE Transactions of Aerospace and Electronic Systems 43(1), 227-238 (2007).
13. Jiang, L. A. and Luu, J. X., "Heterdyne detection with a weak local oscillator," Applied Optics 47(10), 1486-1503 (2008).
14. Winzer, P. J. and Leeb, W. R., "Coherent lidar at low signal powers: Basic considerations on optical heterodyning," Journal of Modern Optics 45(8), 1549-1555 (1998).
15. Goodman, J. W., [Statistical Optics], Wiley, New York, (1985).
16. Carrara, W., Majewski, R. and Goodman, R., [Spotlight Synthetic Aperture Radar: Signal Processing Algorithms], Artech House, Boston, (1995).
17. Richards, P. L., "Bolometers for infrared and millimeter waves," Journal of Applied Physics 76(1), 1-24 (1994).
18. Frenkel, A., Sartor, M. A. and Wlodawski, M. S., "Photon-noise-limited operation of intensified CCD cameras," Applied Optics 36(22), 5288-5297 (1997).
19. Zhou, H., Nemati, B., Shao, M., Schulze, W. and Trahan, R., "Low-Cost Chirp Linearization for Long-Range ISAL Imaging Application," Proc. SPIE 9846, 13 (2016).
20. Bhandari, A., Hamre, B., Frette, O., Zhao, L., Stamnes, J. and Kildemo, M., "Bidirectional reflectance distribution function of Spectralon white reflectance standard illuminated by incoherent unpolarized and plane-polarized light," Applied Optics 50(16), 2431-2442 (2011).
21. Opatrny, T. "Number-phase uncertainty relations," Journal of Physics A: Mathematical and General 28(23), 6961- 6975 (1995).
22. Shapiro, J. H. and Shepard, S. R., "Quantum phase measurement: A system-theory perspective," Physical Review A 43(7), 3795-3818 (1991).
23. Shapiro, J. H. and Wagner, S. S., "Phase and amplitude uncertainties in heterodyne detection," IEEE Journal of Quantum Electronics 20(7), 803-813 (1984).
24. Perinova, V., Luks, A. and Perina, J., [Phase in Optics], World Scientific Publishing, Singapore, (1998).
25. Carruthers, P. and Nieto, M. M., "Phase and angle variables in quantum mechanics," Reviews of Modern Physics 40(2), 411-440 (1968).

Backup Slides

Photon Count Estimation

- Detector DC voltage determines local oscillator photon count:

$$P_L = \frac{V_{DC}}{G_{DC}} \Rightarrow N_L = \frac{P_L \tau}{E_{Ph}}$$

- The mean one sided PSD: (j^{th} voltage measurement in the k^{th} pulse)

$$P_u = \frac{2}{N_V N_P \delta f} \sum_{k=0}^{N_P-1} \left| \sum_{j=0}^{N_V-1} V_{j,k} \exp\left(-i2\pi \frac{ju}{N_V}\right) \right|^2, \quad u = [0, N_V - 1]$$

- The number of photons in each range bin is given by:

$$P_{Het} = \frac{\sqrt{2\delta f \left(P_u - \bar{P}_{BG}\right)}}{G_{AC}} \Rightarrow P_{Ret} = \frac{P_{Het}^2}{4P_L} \Rightarrow N_S = \frac{P_{Ret}\tau}{E_{Ph}}$$

A_d :	Detector area
η_d :	Detector efficiency
e :	Electron charge
G :	Detector Gain
η_h :	Heterodyne efficiency
N_L :	# LO photons per pulse
n :	# measured photons
N_R :	# range bins
N_s :	# signal photons per pulse
h :	Plank's constant
τ :	Pulse time

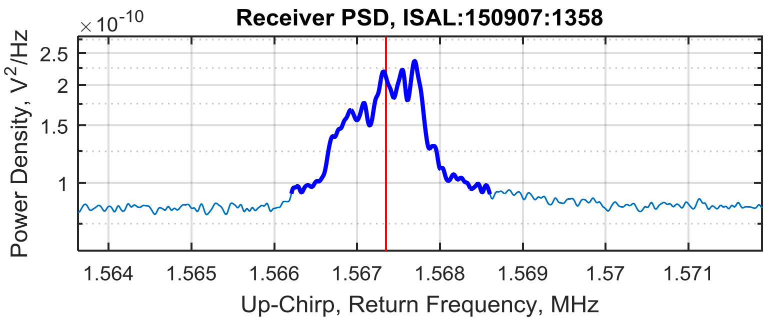

CNR Derivation

Jet Propulsion Laboratory
California Institute of Technology

- Total power at detector due to an E field is related to the mean field amplitude:

$$P_d = \int_{A_d} \frac{1}{2}\left|E\exp(2\pi ift + i\varphi)\right|^2 dA = \frac{hcN}{\lambda\tau} \equiv \frac{1}{2}A_d\bar{E}^2$$
$$\bar{E}^2 = \frac{2hcN}{\lambda A_d \tau}$$

- Detector output current due to single range element:

$$I_d = \frac{\eta_d e}{h\nu}\int_{A_d} \tfrac{1}{2}\left|E_L\exp\left(2\pi i\left(f_0 + \tfrac{1}{2}\dot{f}t\right)t\right) + E_s\exp\left(2\pi i\left(f_0 + \tfrac{1}{2}\dot{f}(t+\Delta t)\right)(t+\Delta t) + i\varphi\right)\right|^2 dA$$
$$= \frac{\eta_d e}{h\nu}\left[\tfrac{1}{2}A_d\bar{E}_L^2 + \tfrac{1}{2}A_d\bar{E}_S^2 + A_d\sqrt{\eta_h}\bar{E}_L\bar{E}_S\cos(2\pi\Delta ft + \varphi_s)\right]$$
$$= \eta_d e\frac{N_L + N_S}{\tau} + 2\eta_d e\frac{\sqrt{\eta_h N_L N_S}}{\tau}\cos(2\pi\Delta ft + \varphi_s)$$

- DFT of 2M samples of I_d at the carrier frequency:

$$D(\Delta f) = \frac{\tau}{2M}\sum_{m=0}^{2M-1} 2\eta_d e\frac{\sqrt{\eta_h N_L N_S}}{\tau}\cos(2\pi\Delta ft_m + \varphi_s)\exp(-2\pi i\Delta ft_m)$$
$$= \eta_d e\sqrt{\eta_h N_L N_S}\exp(i\varphi_s)$$

- Measured quantity is expected number of signal photons plus complex noise:

$$\eta_d\sqrt{\eta_h N_L \tilde{N}_S}\exp(i\varphi) = \eta_d\sqrt{\eta_h N_L N_S}\exp(i\varphi_s) + N(0,\sigma_{SN}^2) + N(0,\sigma_{NEP}^2)$$

- Measurement has a variance due to shot noise:

$$\sigma_{SN}^2 = \eta_d\frac{N_L + N_S}{2} \approx \eta_d\frac{N_L}{2},\quad N_L >> N_s$$

- Measurement has variance due to detector noise

$$\sigma_{NEP}^2 = \frac{1}{2}\left(\frac{P_{NE}\sqrt{\tau^{-1}}\lambda}{hc}\tau\right)^2 = \frac{P_{NE}^2\lambda^2\tau}{2h^2c^2}$$

- CNR is defined as

$$\frac{\text{Estimate of carrier strength}}{\text{StdDev of estimate of carrier strength}}$$

A_d :	Detector area
η_d :	Detector efficiency
e :	Electron charge
G :	Detector Gain
η_h :	Heterodyne efficiency
N_L :	# LO photons per pulse
n :	# measured photons
N_R :	# range bins
N_s :	# signal photons per pulse
h :	Plank's constant
τ :	Pulse time

CNR Derivation (cont.)

Jet Propulsion Laboratory
California Institute of Technology

- CNR is defined as $\dfrac{\text{Estimate of carrier strength}}{\text{StdDev of estimate of carrier strength}}$
- Measurement gives number of detected photons $\tilde{N}_S$.

$$\eta_d\sqrt{\eta_h N_L \tilde{N}_S}\exp(i\varphi) = \eta_d\sqrt{\eta_h N_L N_S}\exp(i\varphi_s) + N(0,\sigma_{SN}) + N(0,\sigma_{NEP}) \qquad \sigma_{SN}^2 \approx \eta_d \frac{N_L}{2} \qquad \sigma_{NEP}^2 = \frac{P_{NE}^2\tau}{2h^2\nu^2}$$

- Second moment gives estimate of $\tilde{N}_S$

$$\mathrm{var}\left(\eta_d\sqrt{\eta_h N_L \tilde{N}_S}\exp(i\varphi)\right) = \mathrm{var}\left(\eta_d\sqrt{\eta_h N_L N_S}\exp(i\varphi_s)\right) + \mathrm{var}\left(N(0,\sigma_{SN})\right) + \mathrm{var}\left(N(0,\sigma_{NEP})\right)$$

$$\langle N_L \tilde{N}_S\rangle = \langle N_L N_S\rangle + 2\frac{\sigma_{SN}^2 + \sigma_{NEP}^2}{\eta_d^2\eta_h}$$

- Fourth moment gives variance of $\tilde{N}_S$

$$\mathrm{var}(\tilde{N}_S) = \langle \tilde{N}_S^2\rangle - \langle \tilde{N}_S\rangle^2 = \frac{4N_S}{\eta_d^2\eta_h N_L}\left(\sigma_{SN}^2 + \sigma_{NEP}^2\right) + \frac{4}{\eta_d^4\eta_h^2 N_L^2}\left(\sigma_{SN}^4 + \sigma_{NEP}^4\right) + \frac{8\sigma_{SN}^2\sigma_{NEP}^2}{\eta_d^4\eta_h^2 N_L^2}$$

$$= \frac{2N_S}{\eta_d\eta_h} + \frac{1}{\eta_d^2\eta_h^2} + \frac{4N_S\sigma_{NEP}^2}{\eta_d^2\eta_h N_L} + \frac{4\sigma_{NEP}^2}{\eta_d^4\eta_h^2 N_L} + \frac{4\sigma_{NEP}^4}{\eta_d^4\eta_h^2 N_L}$$

- $$CNR = \frac{\langle N_L \tilde{N}_S\rangle}{\sqrt{\mathrm{var}(N_L\tilde{N}_S)}} = \frac{N_S}{\sqrt{\dfrac{2N_S}{\eta_d\eta_h} + \dfrac{1}{\eta_d^2\eta_h^2} + \dfrac{4N_S\sigma_{NEP}^2}{\eta_d^2\eta_h N_L} + \dfrac{4\sigma_{NEP}^2}{\eta_d^4\eta_h^2 N_L} + \dfrac{4\sigma_{NEP}^4}{\eta_d^4\eta_h^2 N_L}}}$$

A_d : Detector area
η_d : Detector efficiency
e : Electron charge
G : Detector Gain
η_h : Heterodyne efficiency
N_L : # LO photons per pulse
n : # measured photons
N_R : # range bins
N_s : # signal photons per pulse
h : Plank's constant
τ : Pulse time

An unbiased estimator of N_S is $n - 2\sigma'^2$, since $\langle n - 2\sigma'^2\rangle = s^2 = N_S$. Since, from Eq. (5), σ'^2 = constant, the variance of this estimator is the same as the variance of n. Using the definition given above, the CNR of heterodyne detection for imaging applications is the ratio of N_S to the standard deviation of its estimator:

$$\mathrm{CNR_{IM}} = \frac{N_S}{\sqrt{\dfrac{2N_S}{\eta_d\eta_h} + \dfrac{1}{\eta_d^2\eta_h^2}}} \approx \sqrt{\frac{\eta_d\eta_h N_S}{2}} \quad \text{for } N_S >> 1/(\eta_d\eta_h)$$
$$\approx \eta_d\eta_h N_S \quad \text{for } N_S << 1/(\eta_d\eta_h)\ , \qquad (7)$$

where Eqs. (5) and (6) have been used. Taking $\eta_d = \eta_h = 1$ in the first approximation shows that the best possible CNR of heterodyne detection is a factor of $\sqrt{2}$ below the best possible CNR of direct detection. For $N_S << 1/(\eta_d\eta_h)$, $\mathrm{CNR_{IM}}$ is proportional to the number of photons detected, rather than to the square

R. L. Lucke and L. J. Rickard, "Photon-limited synthetic-aperture imaging for planet surface studies planet surface studies," *Applied Optics*, vol. 41, no. 24, pp. 5084-5095, 2002.

Jet Propulsion Laboratory
California Institute of Technology

Contrast vs Mean & Max CNR